



## Structural concepts for Soltanieh fault zone (NW Iran)

Bitra Javidfakhr<sup>\*1</sup>, Seiran Ahmadian<sup>2</sup>

1. Department of Geology, University of Zanjan, Zanjan, Iran  
2. Cape Consulting Group, N 303, Motahari Avenue, Tehran, Iran

Received 14 August 2018; accepted 2 March 2019

### Abstract

Active deformation in Alborz range is due to N-S convergence between Arabia and Eurasia. This paper provides geomorphic traces of regional deformation in NW Iran in order to characterize active faulting on major faults. Soltanieh and North Zanjan fault systems are involved in convergence boundary extent between South Caspian Basin and Central Iran. Soltanieh and North Zanjan faults are major reverse faults in the study area. Soltanieh fault has been probably responsible for historical Soltanieh earthquake in 1803. Accurate mapping accompanied by field observations enabled offset determination along active faults. We presented geomorphic documents indicating left-lateral strike-slip movements in Soltanieh fault zone. Kinematics is achieved through analyzing inversion results obtained from kinematic measurement sites which are generally scattered along Soltanieh fault zone. Fault kinematic data inversion results (slip-vector measurement in fault planes) indicate a dominant NE trending horizontal maximum stress axis ( $\sigma_1$ ). Kinematic inversion results infer reverse faulting mechanism accompanied by strike-slip component.

**Keywords:** Zanjan, Soltanieh Fault, Earthquake, Quaternary, Offset

### 1. Introduction

Alborz range is bounded from south by Central Iran block. Western Alborz is continued to Talesh Mountains for about 400km. Soltanieh and North Zanjan fault systems running in western Alborz are involved in convergence boundary between South Caspian Basin (SCB) and Central Iran. Zanjan and Takab extents are suggested as seismic gaps inferring a seismically quiet zone in a region that has experienced large earthquakes (see Fahmi et al., 1988; Solaymani Azad et al. 2011). Tectonic activity continues presently in this region (refer to Fig 1 and Table 1). Recent earthquakes which occurred around Zanjan are presented in figure 2. Soltanieh belt is defined as a narrow belt with more than 150km length and maximum 10-12km width by Stocklin and Eftekharneshad (1969). Soltanieh and North Zanjan faults are major faults occurring at longitude between 48.00°E and 49.30°E (refer to Fig 3). Activity of Soltanieh, Zanjan and North Zanjan fault zones are studied in relation to the role of major adjacent faults in regional tectonic pattern considering the large-scale geologic structures. This paper analyzes geomorphic remarks in order to realize active tectonic processes in this structural zone situated in northwest Iran. Most important features in structural units are discussed with considerations about regional Late Cenozoic active faulting. Faults are generally supported by field surveys and kinematic data complemented by geomorphic investigations. There are several sites comprising signals for recent fault activity recorded in Quaternary deposits.

Paleotethys Ocean divided Eurasian Plate from Central Iran blocks in NE Iran while Neotethys Ocean opened in southern boundary of Central Iran blocks during Permian. Iran's tectonic framework is characterized by active convergence between Arabia and Eurasia. Alborz mountain belt is extended in E-W direction as result of Central Iran N-S convergence in Late Triass (Berberian 1983) and SCB movement toward NW in Pleistocene (Ritz et al. 2006). Western Alborz and Talesh structural trends follow Caspian Sea coastline. Zanjan fault system is considered as southern prolongation of Alborz range toward North, connecting Alborz to Talesh Mountains. Zanjan fault system is constituted by active thrusts and dextral strike-slip faults linking toward southeast near Zanjan (Solaymani Azad et al. 2011). The fault zones control structural evolution in southeast termination of Zanjan-Mianeh Basin. Alborz is a seismically active region situated in Alpine-Himalayan seismic belt. Crustal deformation resulted large earthquakes in northern Iran (Nemati et al. 2013; Abdollahzadeh et al. 2014; Nemati 2015). Significant offshore seismicity is observed in 50km wide SCB margin (Aziz Zanjani et al. 2013; Rastgoo et al. 2018). South Caspian basement slab is undergoing severe seismic deformation as it underthrusts beneath northern Talesh (Aziz Zanjani et al. 2013).

This paper presents new structural and geomorphic data in Soltanieh fault zone. Kinematics is achieved by analyzing inversion results achieved from kinematic measurement data in sites generally scattered along Soltanieh fault zone. Seismicity background and geomorphic investigations are discussed in next sections.

\*Corresponding author.

E-mail address (es): [bjavid@znu.ac.ir](mailto:bjavid@znu.ac.ir)

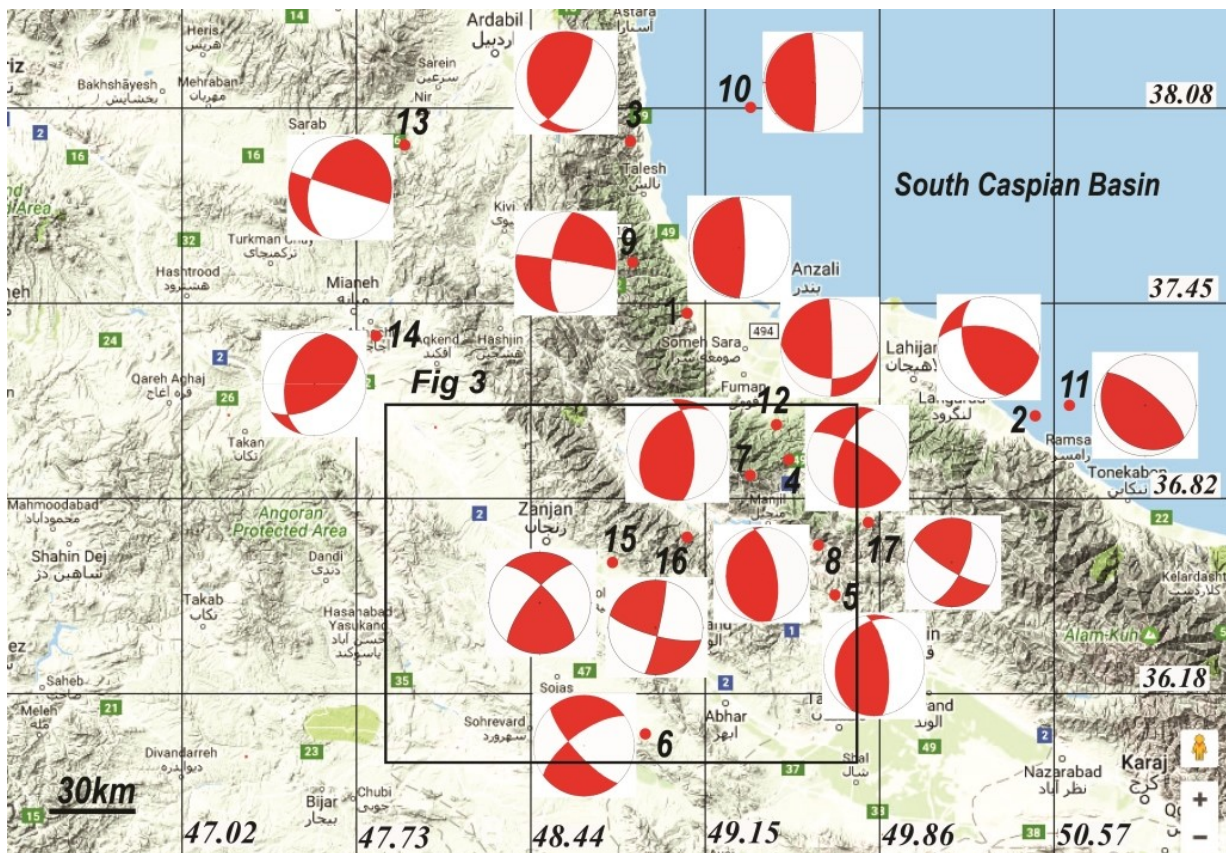


Fig 1. Earthquake locations ( $M \geq 4$ ) surrounding the study area are marked by red circles. Beach-balls indicate earthquake focal mechanisms for each seismic data. Refer to Table 1 for more information. Study area is defined by a rectangle.

## 2. Seismicity

Soltanieh dome in Soltanieh city is an elegant historical monument recorded as UNESCO world heritage site. Neighbouring areas in study region has been subject to several historic earthquakes (Berberian and Yeats 1999; Berberian and Yeats 2001) such as Polrud earthquake ( $M_s \sim 7.2$ ) in 15 August 1485 and Bozqush earthquake ( $M_s \sim 6.7$ ) in 22 March 1879. Berberian (1976) suggested Bozqush fault in Azarbaijan to be linked with Bozqush earthquake which was followed by several aftershocks that ruined district between Nir and Mianeh (Ambraseys 1974). Major destruction occurred in eastern and southeastern slopes of Bozqush Mountains leading to severe damage. This shock was strongly felt in Tabriz and Zanjan. Totally, more than 3200 people were killed.

A historical earthquake reported in Soltanieh in 1803 ( $M > 5.3$  and  $I.7$ ) and Soltanieh fault has been probably responsible for it (Berberian 1976). Historical 1608 April 20 ( $M_s \sim 6.7$ ) Alamutrud earthquake (Berberian 2014) probably occurred along Alamutrud fault. Buin-Zahra earthquake ( $M 7.2$ ) in 1 September 1962 killed more than 20,000 people destructing about 290 villages. Left-lateral strike-slip faulting is reported for

Ipak fault; seismic source for Buin-Zahra earthquake. Changureh (Avaj) earthquake occurred in 22 June 2002 ( $M_w 6.4$ ) in south Qazvin Province causing widespread destruction. Avaj earthquake epicenter corresponds to Buin-Zahra earthquake macro-seismic center. Largest earthquakes recorded in the study area are listed in Table 1. Rezvanshahr earthquake in 1978 ( $M 6$ ), Shaft earthquake in 1983 ( $M 5.6$ ), and Manjil-Rudbar earthquake in 1990 ( $M_w 7.3$ ) are major examples for instrumental seismic events taken up in western Alborz. Manjil-Rudbar earthquake occurred in 20 June 1990 (see Berberian and Walker 2010). The shock was felt in most parts of NW Iran; including Arak, Zanjan and Tabriz. This earthquake destroyed Rudbar, Manjil and Loshan and 700 villages in Sefidrud river valley killing more than 35,000 people. The 2005 September 26, Mianeh earthquake ( $M_l 4.9$ ) occurred in western parts of study area. Another seismic event occurred in 27 May 2008 ( $M_l 5.4$ ) around Yousef Abad in southeast Zanjan (see Mirzaei Alavijeh et al. 2011). Figure 2 is concentrated on latest earthquakes occurred around Soltanieh.

Table 1. Information for earthquake focal mechanism parameters is presented. Nodal planes available for earthquakes are mentioned in the last column. ID numbers refer to beach-ball labels presented in figure 1. Reference for earthquake source parameters is given in abbreviation.

Date (mm/dd/yyyy)	Time (GMT)	Latitude	Longitude	Depth (km)	Magnitude	Reference	ID	Nodal Planes		
								Strike	Dip	Slip
6/24/1903	16:56:00	37.48	48.96		Ms:5.9	AMB				
2/9/1903	5:18:00	36.58	47.65		Ms:5.6	AMB				
1/9/1905	6:17:00	37.00	48.68		Ms:6.2	AMB				
6/17/1948	14:08:31	36.59	49.44		M:5.5	NOW				
4/12/1956	22:34:49	37.33	50.26	30	M:5.5	NOW				
11/4/1978	15:22:23	37.43	49.11	15	Mw:6.3	CMT	1	177 000	09 81	087 090
5/4/1980	18:35:26	38.08	49.41	15	Mw:6.5	CMT	10	179 001	05 85	088 090
7/22/1980	5:17:10	37.15	50.67	30	Mw:5.5	CMT	11	135 310	20 70	095 088
12/3/1980	4:26:14	37.09	50.53	16	Mw:5.3	CMT	2	160 281	52 57	136 047
8/4/1981	18:35:49	37.90	48.84	25	Mw:5.6	CMT	3	159 032	26 73	040 111
6/20/1990	21:00:31	36.95	49.52	15	Mw:7.4	CMT	4	200 300	59 73	160 032
6/21/1990	9:02:19	36.51	49.77	15	Mw:5.7	CMT	5	204 351	26 68	121 076
6/24/1990	9:45:56	36.08	48.91	15	Mw:5.3	CMT	6	234 138	69 75	-163 -022
6/7/1990	19:34:59	37.05	49.48	15	Mw:5.3	CMT	12	094 359	37 86	006 127
11/28/1991	17:20:01	36.88	49.33	15	Mw:5.6	CMT	7	219 354	36 63	130 065
3/2/1997	18:29:45	37.86	47.87	15	Mw:5.3	CMT	13	200 108	41 89	002 131
2/28/1998	12:39:10	36.99	48.76	15	Mb:4.5	EHB				
9/28/1998	17:26:27	36.50	48.70	15	Mb:4.5	EHB				
4/19/2002	13:46:53	36.67	49.74	18	Mw:5.2	CMT	8	183 349	26 64	103 084
9/26/2005	18:57:12	37.36	47.77	20	Mw:5.2	CMT	14	194 057	43 56	055 118
5/11/2006	20:06:45	37.57	48.86	14	Mw:4.8	CMT	9	188 279	67 88	-002 -157
5/27/2008	6:18:04	36.55	48.75	14	Ml:5.4	IIEES	15	317 220	68 72	020 157
9/13/2008	19:24:14	36.78	49.75	7	M: 4.2	ISC				
9/8/2010	5:30:32	36.82	49.44	5	M: 4.3	ISC				
3/18/2012	2:38:15	36.74	49.06	10	M:4.6	ISC	16	013 105	84 76	166 006
5/10/2015	22:08:57	36.73	49.87	5	Mw:4.3	ISC	17	025 121	68 76	165 023
6/30/2015	7:55:29	36.61	49.91	7	M:4.1	ISC				
10/14/2016	19:58:41	36.61	48.78	10	Mb:4.2	ISC				

### 3. Geomorphic investigations

We investigated geomorphic traces of active faulting in order to analyze deformation in Soltanieh fault zone. Precise mapping complemented by field investigations helped offset determination along major faults. In next sections, we analyze structural settings and kinematics

#### 3.1. Soltanieh fault zone

Soltanieh fault zone is a wide brittle shear zone defined by almost parallel fault segments. Soltanieh belt (Ghadimi et al. 2012) is an uplifted Precambrian-Paleozoic basement which includes Precambrian, Paleozoic and Mesozoic Formations. There are extensive open folds with SE plunging axes in widespread Soltanieh range. Folds are asymmetrical with long eastern flanks. Soltanieh fault is NW trending reverse fault which runs nearby Soltanieh which extends

of Soltanieh, Zanjan and North Zanjan faults complemented by detailed geomorphic studies along different fault segments. It is a key area for determining recent behavior of major active faults since there are deformation markers affecting Quaternary deposits.

for more than 130km (see Fig 3). Soltanieh fault characterizes boundary between heights of Kahar, Soltanieh and Barut Formations and Quaternary deposits. Soltanieh fault is running south parallel North Zanjan fault. Pre-Cambrian and Paleozoic Formations are observed along Soltanieh fault while some parts are juxtaposed over Tertiary units which fill Zanjan-Abhar depression. Compression movements were effective in formation of Zanjan-Abhar depression.

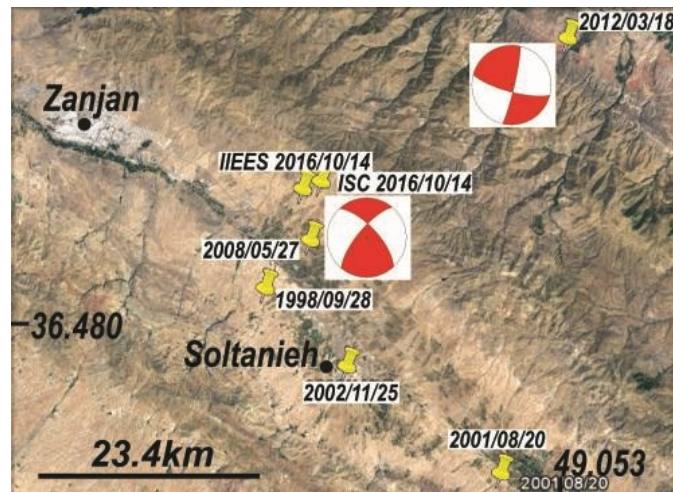


Fig 2. Locations for recent earthquakes around Soltanieh are shown in this image. Seismic event in 2002/11/25 in Soltanieh is not mentioned in Table 1 because its magnitude was small (MI 3.2).



Fig 3. A. Study region structural sketch comprising Manjil, North Zanjan, Soltanieh, Halab and Gheydar faults. Red circles mark fault kinematic measurement sites. Blue circles are fracture measurement sites. Number labels refer to fault kinematic measurement sites defined in Table 2 and figure 15. Alphabet labels refer to fracture measurement sites presented in figure 16.

Figure 4a presents major Soltanieh fault segment around Arjin. Another name for Soltanieh fault is Arjin fault. There is ~15m left-lateral offset recorded over Quaternary features found in west Arjin (Fig 4b). Displacement along Soltanieh fault is concentrated in two sites adjacent Chapdarreh. Figure 4c comprises ~80m left-lateral offset along a fault segment running in southwest Kaboud Gonbad. Figure 4d involves left-lateral offset in order of 70-90m recorded in northeast Tahmasebad. Considering the fault trend, these movements can be representative for Soltanieh fault

actual left-lateral activity. Figure 5a is a broad fault zone outcrop extended in Zanjan-Dandi road. There are minor left-lateral offsets recorded in south Alachaman (Fig 5b). There is ~45m left-lateral offset along active faults affecting Quaternary sediments in Figure 5c. Figure 5d shows several NW trending active fault segments which extend in younger units in north Dourmushqan. Figure 5e involves satellite image for an active fault in southwest Zanjan. This fault is marked by dotted lines. Red asterisk marks related site location for presented photos 5f, 5g and 5h. Kinematic measurements

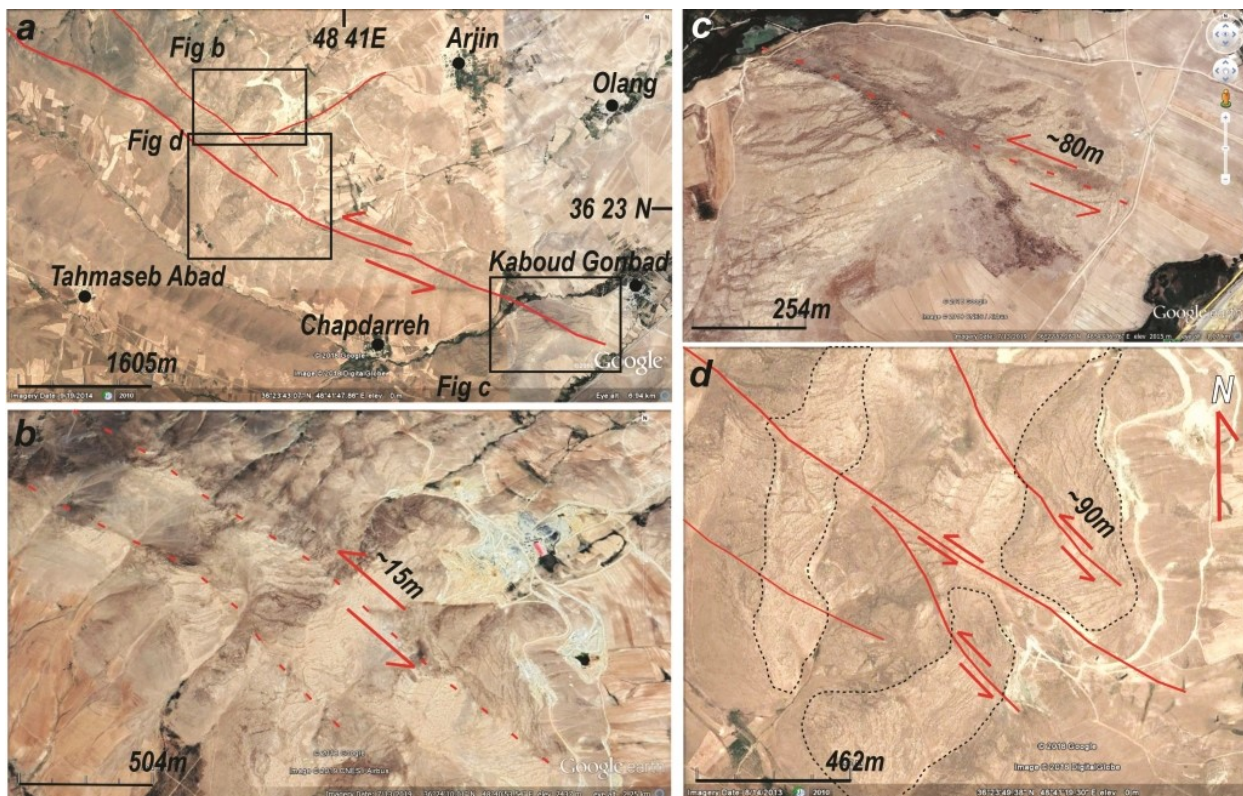


Fig 4. a. Soltanieh fault satellite image comprising left-lateral components in south Arjin. b. There is ~15m left-lateral offset along a minor fault segment. c. We can observe ~80m left-lateral offset in southwest Kaboud Gonbad. d. There are ~90m left-lateral offsets along fault segments affecting Quaternary surfaces.

Kashkabad fault is included in Soltanieh fault zone. This fault is mainly covered with Quaternary deposits. Kashkabad fault which runs in south Kashkabad is WNW trending in eastern segments (Fig 6a) while it has an E-W trending in western segments (Fig 6b). Torkandeh fault is a south dipping thrust fault running nearly parallel with Kashkabad fault (Fig 6b). There are active fault segments comprising left-lateral motions recorded in neighboring sites (Figs 6c, 6d and 6e). They include ~45m (Fig 6d) and ~85m (Fig 6e) left-lateral offsets. Soltanieh fault trace passing Kashkabad is shown in figure 6f. Soltanieh fault zone between Papaei

and Koselar is given in figure 7a. In a neighbouring site we can observe a NW trending reverse fault passing south Rayhan and Bayandor (Fig 7b). Almost parallel active fault segments cut Quaternary units around Ajdahatou (Fig 7c). Field geologic evidence for thrust faulting in Quaternary units is offered in figures 7d and 7e in which the outcrop is situated about Papaei. Figure 7d displays a reverse fault affecting Quaternary sediments that terminates to a fault valley. Figure 7e exhibits an active reverse fault in Quaternary units nearby Papaei. Figure 7f exposes fault trace in a closer view.

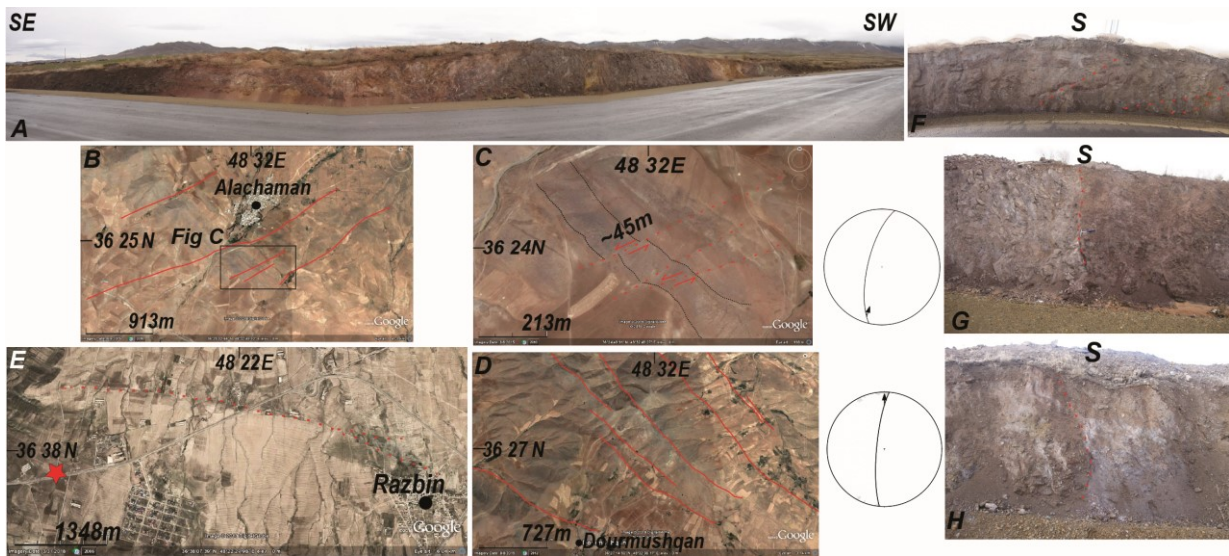


Fig 5. a. This outcrop comprises a broad fault zone in Zanjan-Dandi Road. b. Parallel fault segments in south Alachaman are shown. c. There is ~45m left-lateral offset observed in this satellite image. d. NW trending active fault segments run in Quaternary units in north Dourmushqan. e. Fault zone satellite image in southwest Zanjan. Red asterisk marks site location in 5f, 5g and 5h photos. f. General view from kinematic measurement site. g and h. Faults affecting Quaternary eroded sediments and their right-lateral movements are presented in stereograms.

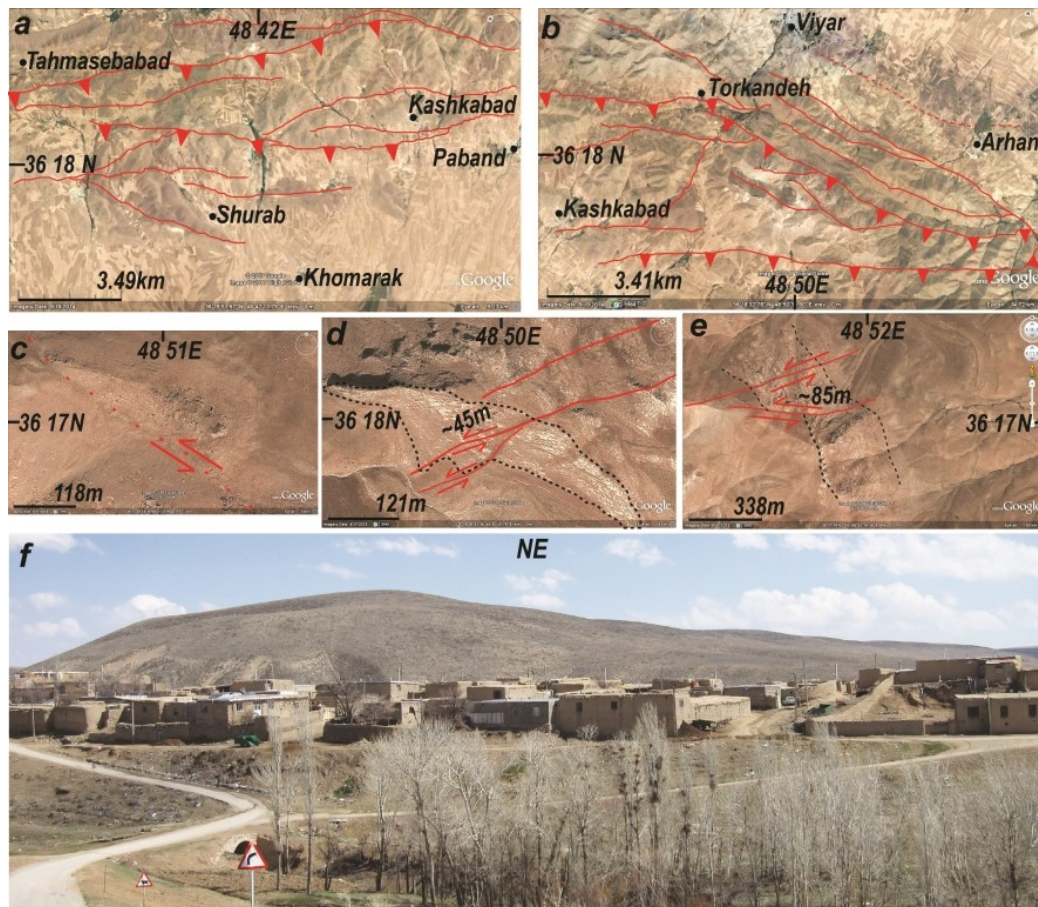


Fig 6. Satellite image related to southern parts of Soltanieh fault zone comprising different fault segments. a. Soltanieh fault in south Tahmasebabad. b. Soltanieh fault in south Torkandeh. c, d and e. Left-lateral offsets recorded in Quaternary units in three neighboring sites. f. Fault trace involved in Soltanieh fault zone passing Kashkabad.

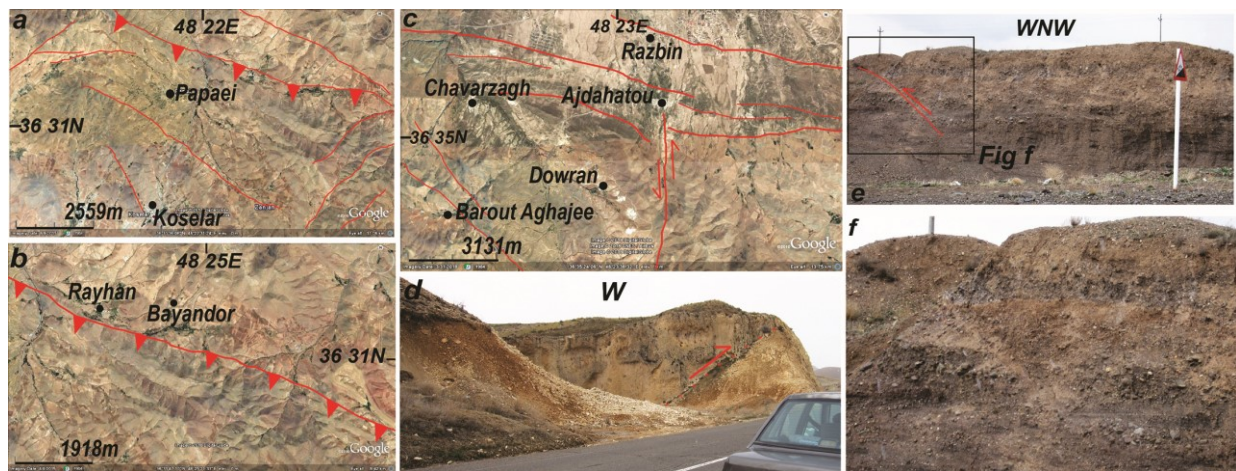


Fig 7. a. Soltanieh fault zone satellite image in area between Papaiei and Koselar. b. A reverse fault segment passing south Bayandor and Rayhan. c. Different fault segments affecting Quaternary units in east Chavarzagh. d. An active reverse fault which terminates to a fault valley. e. Active reverse fault in Quaternary units found in a site around Papaiei. f. Fault plane in close view is presented.

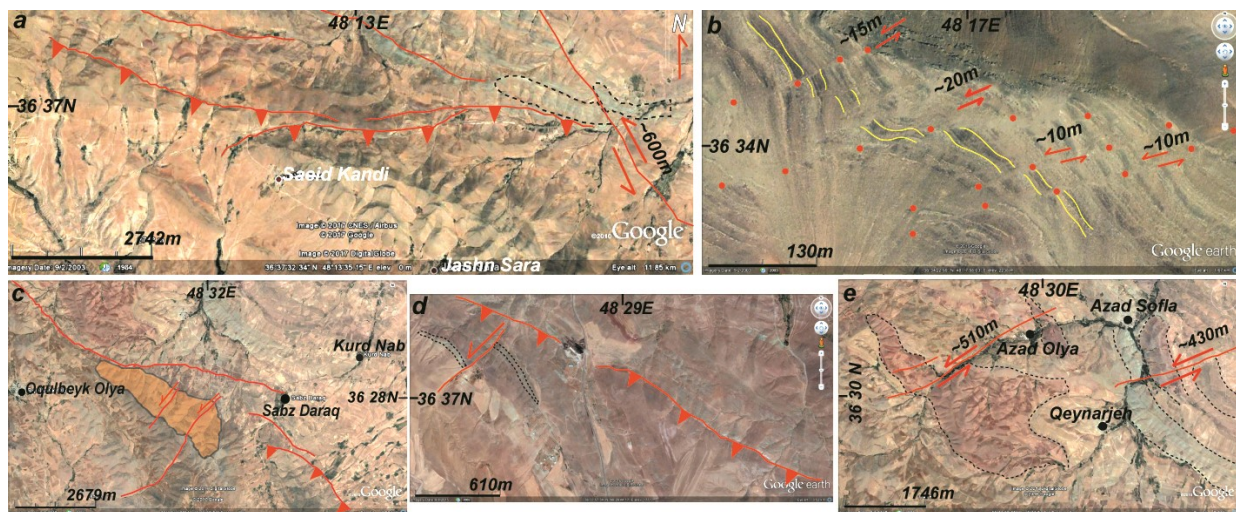


Fig 8. a. Google earth image for area located in north Saaid Kandi. b. Total ~55m left-lateral offset along minor fault segments near Aghkand. c. Thrust and minor strike-slip fault segments in the extent between Oqulbeyk Olya and Sabz Daraq. d. South-dipping reverse fault accompanied by a minor left-lateral strike-slip fault segment in left corner of image. Displaced veins are mentioned. e. There are about 430m and 510m left-lateral offsets along different fault segments in north Qeynarjeh.

Figure 8a displays an E-W trending reverse fault in north Saaid Kandi. There is ~600m left-lateral offset observed in a minor NNW trending fault segment in figure 8a right corner. Approximately parallel left-lateral fault segments comprise total about 55m offset (Fig 8b) in a site situated besides Aghkand. Soltanieh fault zone satellite image in two neighbouring sites are analyzed (Figs 8c and 8e). There are minor NE trending left-lateral strike-slip fault segments affecting older structures in east Oqelbeyk Olya (Fig 8c). There are about 430m and 510m left-lateral offsets observed in adjacent fault segments in north Qeynarjeh (Fig 8e). Figure 8d includes NW trending fault segments in this zone. A minor left-lateral fault offset is seen in left

corner of figure 8d considering mentioned displaced veins. Soltanieh fault zone western termination reaches Mirjan. Figure 9a exposes panoramic photo of an active fault passing Mirjan in contact between mountains and Quaternary plains. Figure 9b defines ~450m right-lateral offset along a minor NE trending fault segment extending between Khalifeh Hesar and Darsajin. Qare Aghaj fault trace is mapped in figure 9c. An earthquake occurred in 1990/06/24 (Mw. 5.3, see Table 1) in ~7km southwest Qezilja. Qare Aghaj fault was probably responsible for this fault considering its proximity to earthquake epicentre and available earthquake focal mechanism. Refer to label 6 in figure 1 and ID number 6 in Table 1 for details.

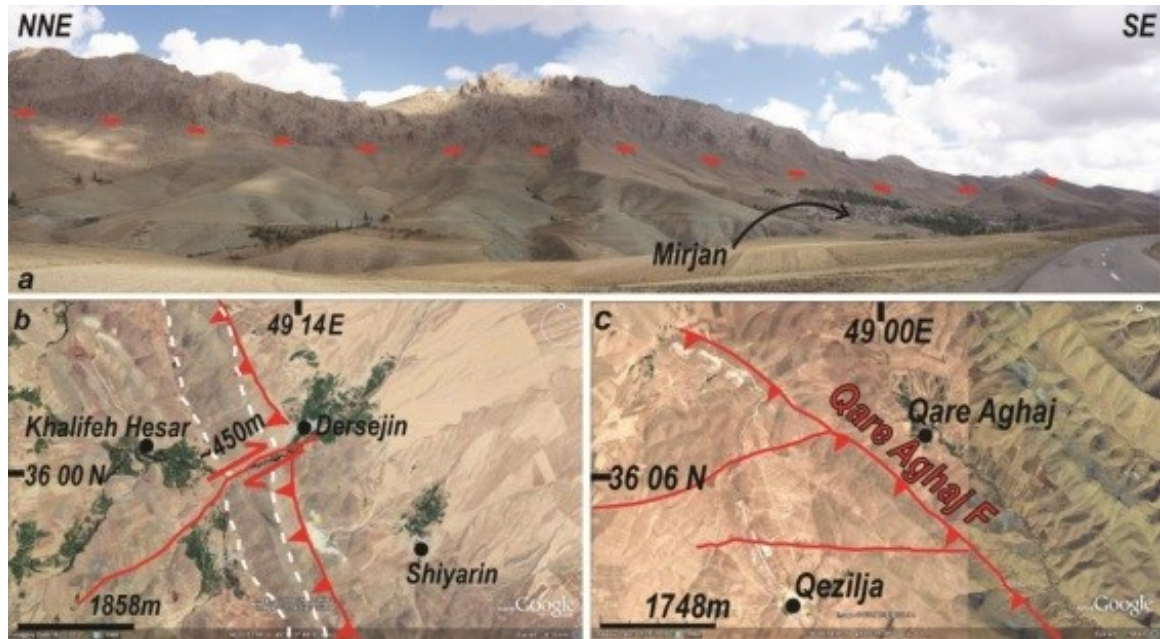


Fig 9. a. Panoramic photo representing Soltanieh fault zone western termination passing Mirjan. b. This image includes Soltanieh fault eastern termination zone, concentrating on minor NE trending fault segment which involves ~450m right-lateral offset. c. Qareh-Aghaj fault situated in Soltanieh zone eastern termination is mapped. An earthquake occurred in 1990/06/24 (Mw. 5.3) in ~7km southwest Qezilja.

### 3.2. Zanjan fault system

Northern and western termination of Zanjan fault system including Kordkandi, Yengejeh, Kenavand and North Jahand-Daghi fault zones are studied (Solaymani Azad et al. 2011). They defined NW trending Yengejeh-Boluk and Kenevand-Baghlujah fault zones situated in northwest Zanjan. Jahand-Daghi range is situated in west Zanjan and Kordkandi zone is included in North Zanjan fault zone. We have briefly analyzed two major fault zones in this fault system including Zanjan and North Zanjan fault zones considering the proximity to Soltanieh fault zone. The mentioned fault zones can superimpose significant seismic hazard to Zanjan. North Zanjan fault (Allen et al. 2011; Solaymani Azad et al. 2011; Toori and Seyitoglu 2014; Salmanlu 2015; Jafari and Rostamkhani 2017) is running parallel Soltanieh fault for more than 80km. Qezel-Owzan River drains into Caspian Sea. Most outcrops in Zanjan region compose Eocene pyroclastic rocks of Karaj Formation. Pyroclastic rocks in northern parts compose green tuffs with limestone interlayers. North Zanjan fault's eastern segment is NW trending while western segment is NNW trending. Eocene igneous and volcanic rocks are thrust over Neogene and Quaternary deposits. Southeast termination of this fault is bounded with Takestan fault, while NW termination links with Mianeh fault. Sohrain, Homayoun, Armaghankhaneh, Taham and Morvarid faults are recognized active faults involved in North Zanjan fault zone.

Figure 10a is a site situated in Zaker-Sorkhe Dizaj road. Measured fault plane and fault gouge are presented in figure 10b. Fault striations representing reverse right-lateral movement is specified in figure 10c. Another geologic fault photo in this road is offered in figure 10d which comprise reverse movements. Figure 10e displays an ENE trending fault affecting older rock units. Kinematic measurement presented in this figure indicates left-lateral motion. Morvarid fault is an active NNE trending fault which runs for ~20km in northeast Zanjan. Morvarid fault has been probably responsible for 2016/10/14 earthquake due to its proximity to earthquake epicentre (Fig 11a). An earthquake occurred in 1998/09/28 (Mb.4.5, see Table 1) in ~8km southeast Ardin. The focal mechanism for this earthquake is not available. Earthquake epicenter is located beside an active fault segment which is mapped in figure 11b. This seismic event happened about 7km southwest of Yousef Abad. Figure 11c shows earthquake epicentre for 2001/08/20 event (Ml 4.1) which is situated along an active fault segment in west Pir Saqqa. Field observations confirm occurrence of North Zanjan fault environs Zaker (Fig 12a). Field geologic data and kinematic measurements for reverse (Fig 12e) and reverse right-lateral faulting process (Fig 12b) in two adjacent sites close to Zaker are offered. Figure 12f is enlargement of the rectangle mentioned in figure 12a in close view which represents layers displaced by normal fault.

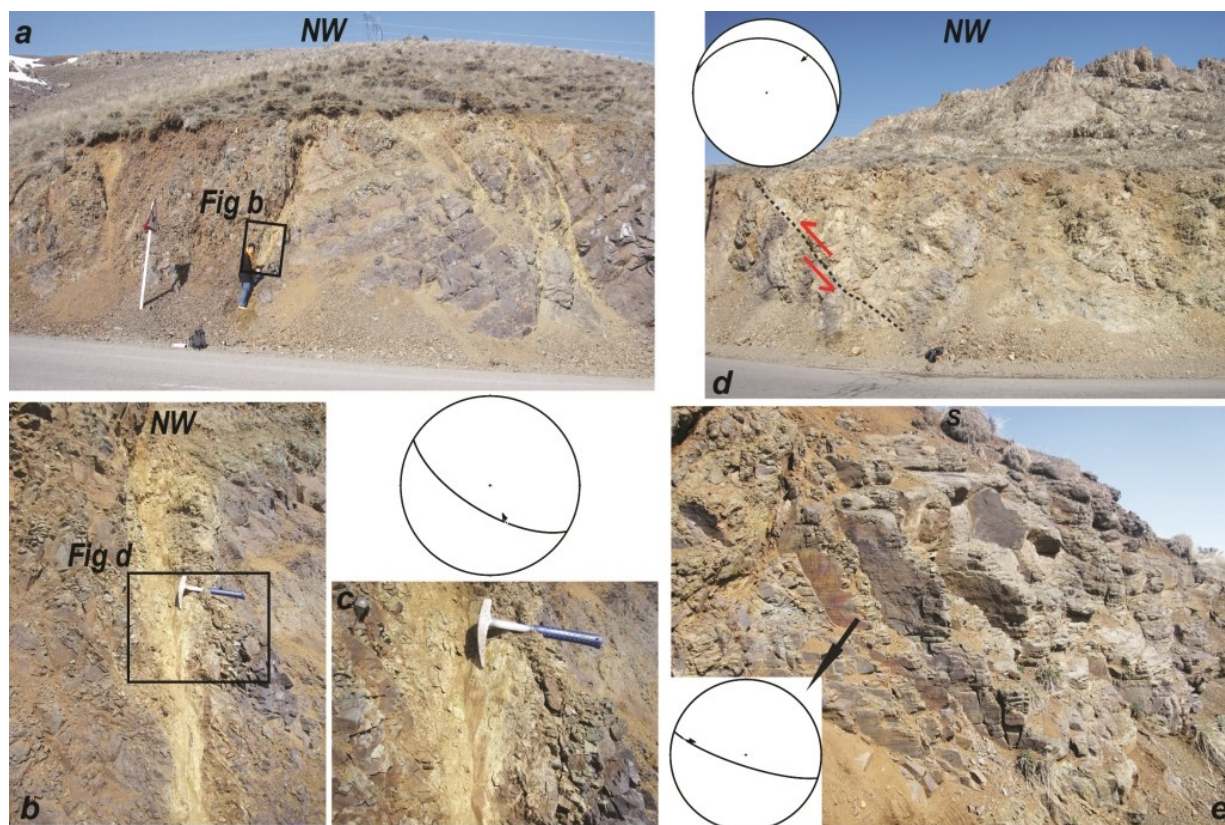


Fig 10. a. This site is situated in Zaker-Sorkkeh Dizaj road. b. Mentioned rectangle in figure 10a is enlarged to clarify measured fault plane. c. Fault plane and reverse dextral movement is specified in stereogram. d. A reverse fault outcrop about Zaker. e. Another measurement site in Zaker-Sorkkeh Dizaj road. Kinematic measurement indicates left-lateral reverse movement.

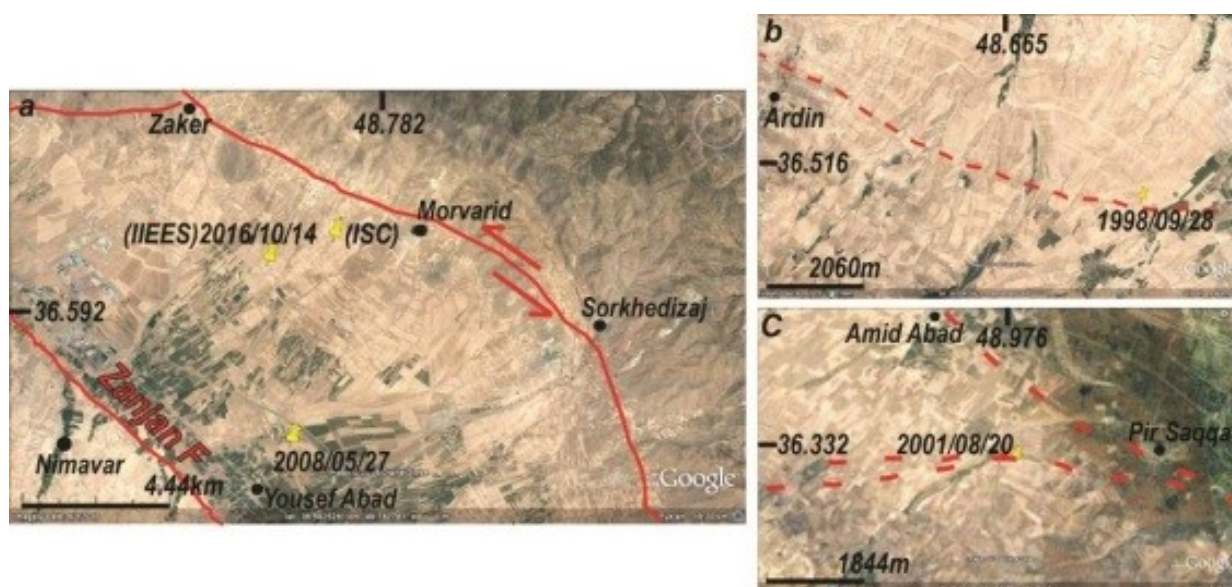


Fig 11. a. Two recent earthquakes occurred in west Morvarid and north Yousef Abad. The epicenter reported for earthquake in 2016/10/14 (Mb 4.2) is presented based on ISC and IIEES databases. b. An earthquake occurred in 1998/09/28 (Mb. 4.5) in ~8km southeast Ardin. This epicenter is situated along the mapped active fault segment. c. Epicentre of earthquake in 2001/08/20 (Ml 4.1) is situated along an active fault segment in west Pir Saqqa.

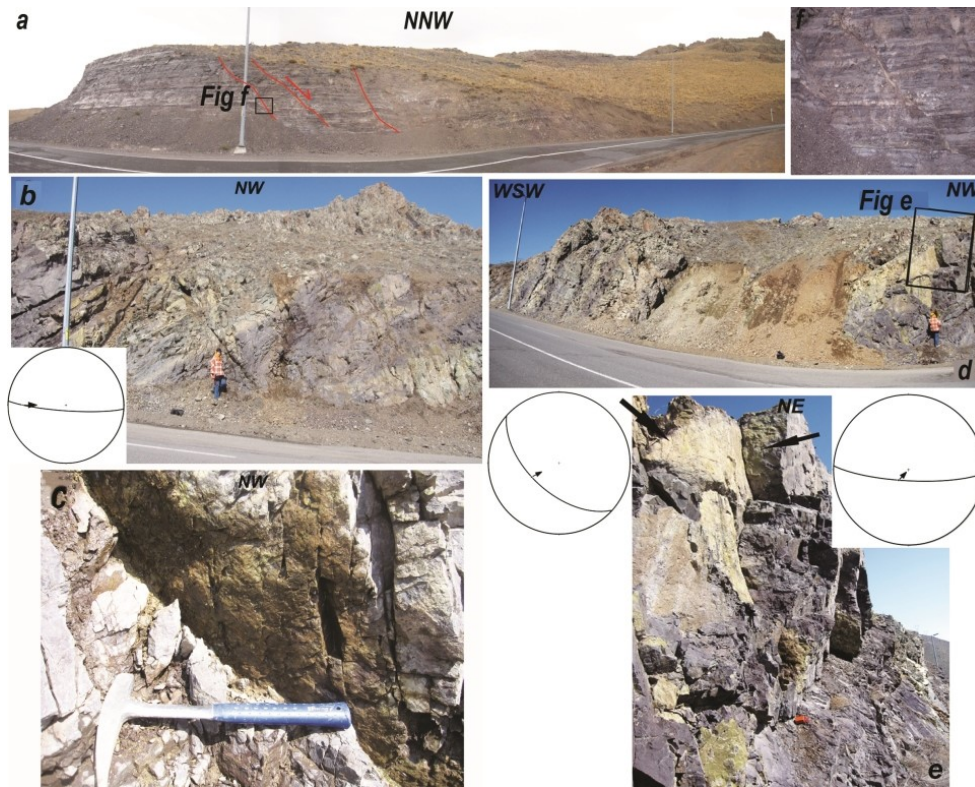


Fig 12. a. North Zanzan fault view near Zaker. b. Geologic evidence for faulting process and measured dextral reverse faults. c. Fault steps indicating right-lateral faulting mechanism. d. Kinematic measurement site adjacent the former site. e. Rectangle in right corner of photo is enlarged in this image. Stereograms comprise fault kinematics measured in parallel planes in lower elevation. Both of fault planes involve reverse movements. f. This photo shows fault close view indicating normal fault movement.

North Zanzan fault segments are mapped in figures 13a and 13b. Figure 13b shows North Zanzan fault trace around Zanzan. An active reverse fault which cuts Quaternary deposits is observed in figure 13c. This site

is situated adjacent Palito. Figure 13d presents this photo in a closer view. Figure 13e shows a thrust fault affecting Quaternary units found around Homayoun. Palito and Homayoun villages are cited in figure 13b.

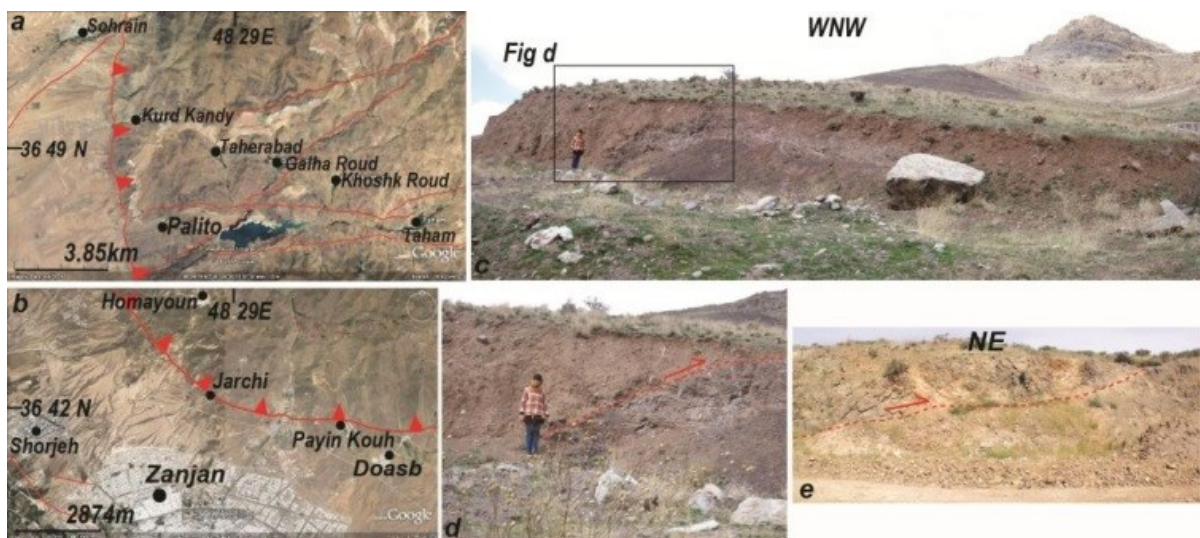


Fig 13. a. Satellite image comprising an active segment of North Zanzan fault. b. North Zanzan fault trace. C and d. Active reverse faulting in a site about Palito affecting Quaternary sediments. e. Thrust fault affecting Quaternary units around Homayoun.

A part of Zanjan fault trace is mapped in figure 14a. This active fault runs in south Zanjan and affects Quaternary river beds. These active fault segments can be assumed as potential danger for Zanjan city considering their proximity. There are active minor reverse fault segments in south Sayan (Fig 14b). Figure

14c includes satellite image of south Zanjan region. NE trending fault segment in this area assigns for ~60m (Fig 14d) left-lateral offset. There is confirmation for ~15m left-lateral offset considering displaced qanats in a site located in north Salmanlou which is offered in figure 14e.

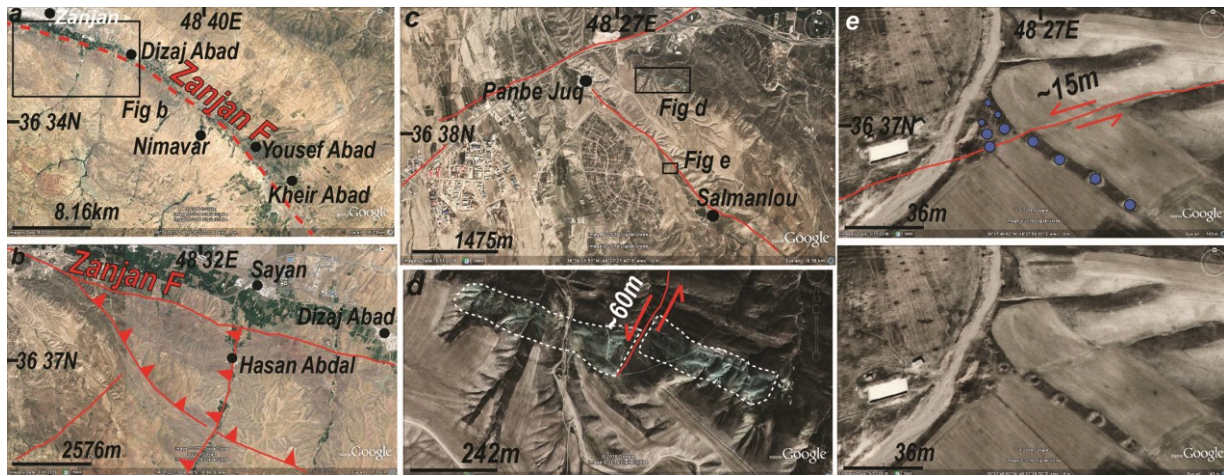


Fig 14. a. Eastern part of Zanjan fault trace is shown in this satellite image. b. Mentioned rectangle in Fig 14a is enlarged to clarify two minor thrusts in southeast Zanjan. c. Satellite image related to the area situated in south Zanjan. d. There is ~60m left-lateral offset observed along a minor fault segment in east Panbe Juq. e. There is ~15m left-lateral offset considering deflected qanats in northwest Salmanlou.

#### 4. Fault kinematic data inversion

Determined slip vector applying striations on a fault plane is usually considered as mechanically defined by a computed stress deviator when the deviation angle is less than 20° (Carey 1979). Deviation angle is defined as the angle between calculated slip vector and the observed striations. Stress inversion results are generally considered to be reliable if 80 percent of deviation angles are less than 20° and if computed solution is stable. We measured several fault slip striations in scattered kinematic measurement sites presented by numeral labels in figure 3.

Table 2 involves fault kinematic inversion results including stress parameters ( $\sigma_1$ ,  $\sigma_2$  and  $\sigma_3$  axes) as well as stress ratio value (R) determined by inversion

method. Large arrows in figure 15 represents azimuth of  $\sigma_1$ . Fault kinematic measurements were scattered generally along Soltanieh fault zone (Fig 3). Along this fault zone, kinematic inversion results imply dominant reverse faulting mechanism accompanied by strike-slip component (Fig 15, sites number 1, 3, 4 and 5). Kinematic results (Fig 15, sites number 1, 2, 4 and 5) define tectonic setting characterized by NE-trending horizontal maximum stress axis ( $\sigma_1$ ). Kinematic measurement in site number 3 (Fig 15) indicates NNW-trending  $\sigma_1$  stress axis with dominant reverse faulting component. This stress regime is probably older than others and such local perturbations in stress state can be due to structural complexities.

Table 2. Fault kinematic inversion results include stress parameters ( $\sigma_1$ ,  $\sigma_2$  and  $\sigma_3$  axes) accompanied by stress ratio value (R) determined by inversion method. N is number of fault planes involved in calculating inversion solutions.

Site	Longitude	Latitude	$\sigma_1$ (trend/plunge)	$\sigma_2$ (trend/plunge)	$\sigma_3$ (trend/plunge)	N	R
1	48.55	36.48	237/27	354/42	125/36	6	0.244
2	48.93	36.78	262/72	100/18	008/05	10	0.444
3	48.47	36.43	170/08	078/16	285/72	5	0.354
4	49.03	36.12	068/10	336/07	212/77	5	0.555
5	48.34	36.62	050/43	154/14	258/43	5	0.192

Some fractures are also measured in different sites in study region which are mentioned by alphabet labels in figure 3. Geometric illustration for fracture planes are presented in figure 16. In each site, N specifies the number of measured fracture data. We measured totally 110 fractures in this region. The geometry of

fracture planes is influenced by several variables and the most important factors in this context include the rock material and thickness of layers and fracture attitude respect to major structures such as folds and faults.

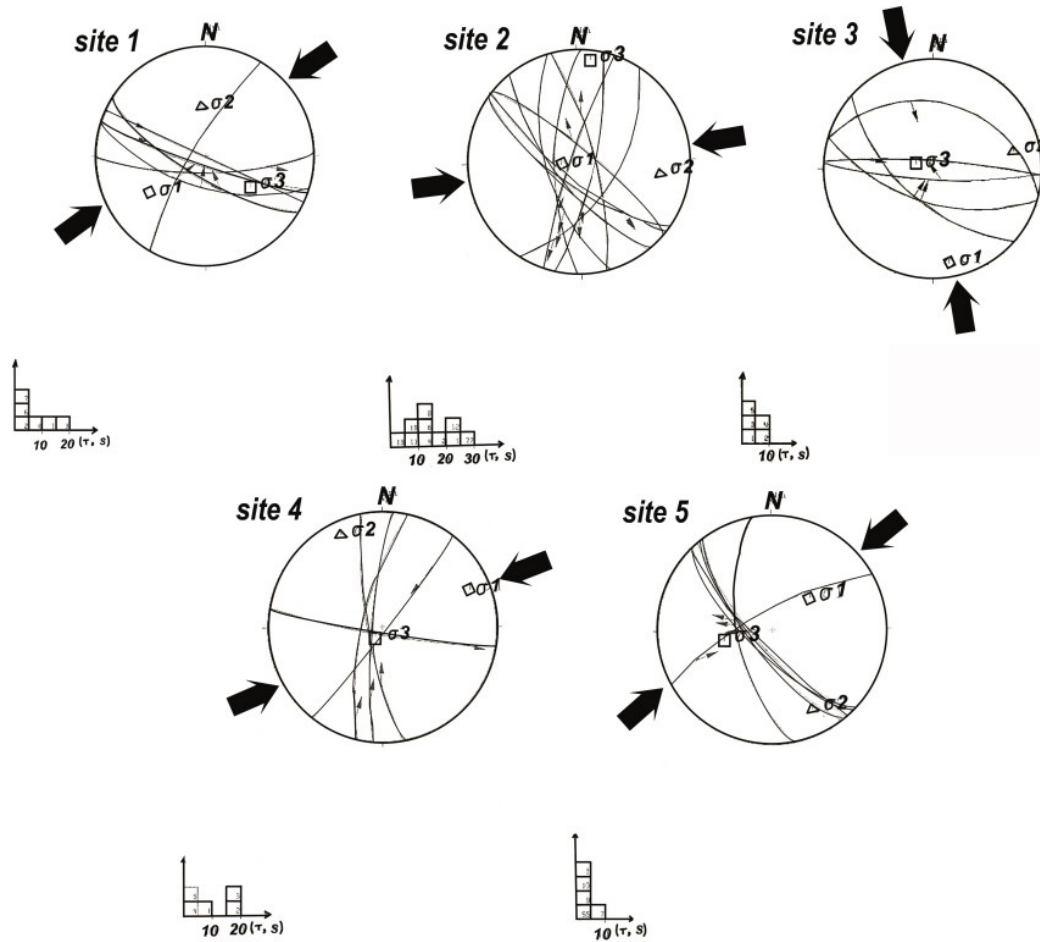


Fig 15. Stereograms comprising kinematic inversion results summarized in Table 2. Number labels refer to site locations given in figure 3. Large arrows indicate maximum stress axis ( $\sigma_1$ ) trend. Fault kinematic inversion results include stress parameters ( $\sigma_1$ ,  $\sigma_2$  and  $\sigma_3$  axes) determined using inversion method (Carey 1979).

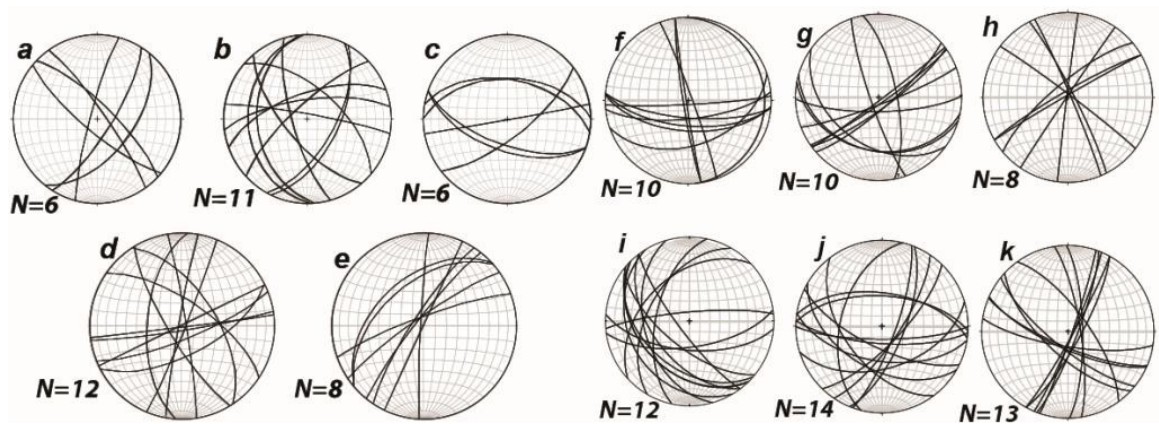


Fig 16. Stereograms represent measured fracture planes. Alphabet labels refer to measurement sites in Fig 3. N is number of measured fracture data.

## 5. Discussion

Arabia-Eurasia plate convergence resulted in forming of complex features in Iranian crust. Late Cretaceous to Paleocene compression occurred along Neotethys margin led to folded and faulted Cretaceous sequences (Stocklin and Eftekharneshad 1969; Stocklin 1974; Stocklin and Setudehnia 1977). Geodetic studies implied N-S shortening across Alborz occurring at  $5 \pm 2$  mmyr<sup>-1</sup> and left-lateral shear across overall belt with  $4 \pm 2$  mmyr<sup>-1</sup> velocity rate (Djamour et al. 2010). A change is proposed for Arabia motion toward Eurasia from NE to N at ~20Ma integrated with drop in plate convergence rates (McQuarrie et al. 2003). Iran accommodates relatively rapid shear strain due to Arabian plate motion toward Eurasia. This motion is associated with lateral convergence change from continental collision in west to oceanic subduction in east (Kaviani et al. 2009). Geologic and geophysic data represented dextral shear in eastern Kura Depression in Azarbaijan and Talesh (e.g. Kadirov and Gadirov 2014). N-S trending Talesh mountain range is a bended fold and thrust belt in Alborz westward continuation.

Ongoing deformation in the study region is due to N-S convergence between Arabia and Eurasia. Transpressional deformation along Alborz southern flank appears to accommodate major transpression part across western Alborz (Guest et al. 2006; Guest et al. 2007). Kinematic change in central Alborz southern boundary can be due to a regional change in stress direction inflection (Ballato et al. 2013). They interpreted the change in structural pattern across a transpressional duplex in southwest Alborz at about 7-6 Ma to reflect mostly strike-slip faulting movements. They concluded ~7-6 Ma deformation pulse should predate SCB westward motion. Crustal shortening and thickening processes could have led to northern Iranian plateau vertical growth, getting a lateral extent similar to present-day not earlier than 10.7Ma (Ballato et al. 2016). The SCB southwest margin and Talesh Mountains are seismically active districts (Aziz Zanjani et al. 2013). The occurrence of numerous earthquakes confirms the existence of intraplate deformation during Late Quaternary in western Alborz.

Soltanieh belt maintains Precambrian, Paleozoic and Mesozoic Formations similar to Alborz zone inferring that they have formed one sedimentary basin from Precambrian until the end of Jurassic (Babakhani and Sadeghi 2005; Ghadimi et al. 2012). Shahmirzae Jeshvaghani and Darijani (2014) applied numerical algorithm for a real data set providing recovery model for shallow high mineralized crustal setting in Soltanieh. Allen et al. (2011) suggested about 15km total right-lateral offset in older rocks within Soltanieh range.

Mahnesan-Mianeh Cenozoic sedimentary basin was affected through post-Miocene deformation. North Zanjan fault has evidence for Late Quaternary activity and probably contains right-lateral component.

Zanjan-Mianeh basin will close most likely in the next millions years (Solaymani Azad et al. 2011). They concluded that Zanjan fault system can cause serious seismic hazard for Zanjan city and surrounding regions. Generally, major NW trending faults in Zanjan fault system involve reverse motions. We can consider them as continuation of right-lateral North Tabriz fault system in a regional context. Earthquake parameters in Alborz mountain range is estimated using a generalized inversion method (Zafarani et al. 2012). Zanjan domain is extended between two different left-lateral western Alborz fault systems (e.g. Manjil-Rudbar fault zone) and right-lateral Azarbaijan fault systems (Solaymani Azad et al. 2019). There are left-lateral strike-slip and thrust movements in Manjil-Rudbar fault zone (Javidfakhr and Ahmadian 2018). North Bozghush fault zone is extended as a dextral strike-slip fault system involving reverse component (Saber et al. 2018). Maragheh and Salmas fault zones are right-lateral strike-slip faults situated in northwest Iran (Taghipour et al. 2018). We can give reference to four destructive earthquakes in Tabriz in 634, 1441, 1522 and 1780 (Berberian and Arshadi 1976) and Salmas earthquake in 1930 (M 7.2) among the most important earthquakes occurred in Azarbaijan. Active faults such as North Tabriz and Bostanabad faults accompanied by Manjil-Rudbar fault system and Salmas and Urmia faults caused northwest Iran to be an active seismic zone in the Middle East.

## 6. Conclusion

There are reverse strike-slip movements observed in the study area corresponding to recent activities of Soltanieh, Zanjan and North Zanjan faults. Soltanieh fault has been probably responsible for historical Soltanieh earthquake in 1803. There are several recent earthquakes reported around Soltanieh and Zanjan (Fig 2) representing the fault zones activity. The probable responsible fault for relatively large seismic events ( $M \geq 4$ ) occurred in study region in 1998, 2001, 2008, and 2016/10/14 is mapped in satellite images. Historical and instrumental earthquakes recorded in northwest Iran confirms necessity to evaluate seismic hazard posed by regional active faults. Soltanieh fault zone includes geomorphic features such as displaced alluvial fans, offset streams and displaced qanats suggesting recent fault activity in this region. Active fault segments traces affecting Quaternary deposits were precisely mapped in satellite images. Major geomorphic features in study area provide reliable schematic pattern to understand how changes in kinematic regime affected this area. There are data achieved from geomorphic surveys and kinematic measurements accompanied by field observations. We presented geomorphic sites indicative for left-lateral strike-slip movements in Soltanieh fault zone. There are ~80m (Fig 4c) and ~90m (Fig 4d) left-lateral offsets recorded in Quaternary units along Soltanieh fault and these movements can be indicative for Soltanieh fault activity considering the fault trend.

Geomorphic features and their associations with fault-related landscapes indicate that Soltanieh and Zanjan fault zones have relatively high level of tectonic activity influenced by dominant compressional forces in this region. Compressional forces are due to Arabian plate movement toward Iranian plateau which resulted in forming NW trending structures in this region.

Kinematics is achieved by analyzing inversion results taken from kinematic measurement sites generally scattered along Soltanieh fault zone. These kinematic inversion results indicate reverse dominant faulting mechanism accompanied by strike-slip component. The modern stress field is characterized by dominant NE trending horizontal maximum stress axis ( $\sigma_1$ ). Integrated geomorphic and structural characteristics suggest coeval reverse and strike-slip faulting mechanism for ongoing activity. There are numerous fracture planes measured in different sites scattered in the study area. Available data is useful to resolve tectonic activity in Soltanieh and Zanjan districts; raising our knowledge about regional tectonic framework in western Alborz.

## References

- Abdollahzadeh Gh, Sazjini M, Shahaky M, Zahedi Tajrishi F, Khanmohammadi L (2014) Considering potential seismic sources in earthquake hazard assessment for Northern Iran, *Journal of Seismology* 18: 357–369.
- Allen M, Jackson J, Walker R (2004) Late Cenozoic reorganization of the Arabia- Eurasia collision and the comparison of short-term and long term deformation rates, *Tectonics* 23, TC2008.
- Allen MB, Kheirkhah M, Emami H, Jones SJ (2011) Dextral shear across Iran and kinematic change in the Arabia–Eurasia collision zone, *Geophysical Journal International* 184: 555-574.
- Ambraseys NN (1974) Historical seismicity of Iran. In materials for the study of seism tectonics of Iran, North Central Iran, *Geological Survey of Iran* 29: 47-116.
- Aziz Zanjani A, Ghods A, Sobouti F, Bergman E, Mortezaejad Gh, Priestley K, Madanipour S, Rezaeian M (2013) Seismicity in the western coast of the South Caspian Basin and the Talesh Mountains, *Geophysical Journal International* 195: 799–814.
- Babakhani AR, Sadeghi A (2005) Geological map of Zanjan. *Geological Survey of Iran*, scale 1:100,000.
- Ballato P, Stockli DF, Ghassemi MR, Landgraf A, Strecker MR, Hassanzadeh J, Friedrich A, Tabatabaei SH (2013) Accommodation of transpressional strain in the Arabia-Eurasia collision zone: new constraints from (U–Th)/He thermochronology in the Alborz mountains, north Iran, *Tectonics* 32: 1–18.
- Ballato P, Cifelli F, Heidarzadeh Gh, Ghassemi MR, Wickert AD, Hassanzadeh J, Nivet GD, Balling Ph, Sudo M, Zeilinger G, Schmitt A, Mattei M, Strecker MR (2016) Tectono-sedimentary evolution of the northern Iranian plateau: insights from middle–late Miocene foreland-basin deposits, *Basin Research* 29 (4): 417-446.
- Berberian M (1976) Documented earthquake faults in Iran, *Geological Survey of Iran*, 39: 143-186.
- Berberian M, Arshadi S (1976) On the evidence of the youngest activity of the North Tabriz fault and the seismicity of Tabriz city. *Geological Survey of Iran*, 39: 397-418.
- Berberian M (1983) The southern Caspian: a compressional depression floored by a trapped, modified oceanic crust, *Canadian Journal of Earth Science* 20: 163–183.
- Berberian M, Yeats RS (1999) Patterns of historical earthquake rupture in the Iranian Plateau, *Bulletin of the Seismological Society of America* 89: 120–139.
- Berberian M, Yeats RS (2001) Contribution of archeological data to studies of earthquake history in the Iranian Plateau, *Journal of Structural Geology* 23: 563–584.
- Berberian M, Walker R (2010) The Rudbar Mw 7.3 earthquake of 1990 June 20; seismotectonics, coseismic and geomorphic displacements, and historic earthquakes of the western ‘High-Alborz’, Iran, *Geophysical Journal International* 182: 1577–602.
- Berberian M (2014) Earthquake and Coseismic Surface Faulting on the Iranian Plateau, a historical, social and physical approach, *Elsevier BV of Radarweg 29, 1034 NX Amsterdam, Netherlands*, 778.
- Carey E (1979) Recherche des directions principales de contraintes associées au jeu d'une population de failles, *Revue Géographie Physique Géologie Dynamique* 21: 57–66.
- Djamour Y, Vernant Ph, Bayer R, Nankali MR, Ritz JF, Hinderer J, Hatam Y, Luck B, Lo Moigne N, Sedighi M, Khorrami F (2010) GPS and gravity constraints on continental deformation in the Alborz mountain range, Iran, *Geophysical Journal International* 183: 1287-1301.
- Fahmi KJ, Ayar, BS, Hassan, IA (1988) The Takab seismic gap-forecasting a major earthquake occurrence off northeastern Iraq, *Journal of Geodynamics* 10 (1): 43-72.
- Ghadimi A, Izadyar J, Azimi S, Mousavizadeh M, Eram M (2012) Metamorphism of Late Neoproterozoic-Early Cambrian schists in southwest of Zanjan from the Soltanieh belt in northwest of Iran, *Journal of Sciences, Islamic republic of Iran* 23 (2): 147-161.
- Guest B, Axen GJ, Lam PS, Hassanzadeh J (2006) Late Cenozoic shortening in the west-central Alborz Mountains, northern Iran, by combined conjugate

- strike-slip and thin-skinned deformation, *Geosphere* 2 (1): 35-52.
- Guest B, Horton BK, Axen GJ, Hassanzadeh J, McIntosh WC (2007) Middle to Late Cenozoic basin evolution in the western Alborz Mountains: Implications for the onset of collisional deformation in northern Iran, *Tectonics* 26, TC6011.
- Jafari H., Rostamkhani A (2017) Geomorphic evidence for Armaghankhaneh and Taham faults, *Journal of Applied researches in Geographical Sciences*, 16 (43): 149-173.
- Javidfakhr B, Ahmadian S (2018) Geomorphic and structural assessment of active tectonics in NW Alborz, *Geopersia* 8 (2): 261-278.
- Kadirov FA, Gadirov AH (2014) A gravity model of the deep structure of South Caspian Basin along submeridional profile Alborz–Absheron Sill, *Global and Planetary Change* 114: 66-74.
- Kaviani A, Hatzfeld D, Paul A, Tatar M, Priestley K (2009) Shear-wave splitting, lithospheric anisotropy, and mantle deformation beneath the Arabia-Eurasia collision zone in Iran, *Earth and Planetary Science Letters* 286: 371–378.
- McQuarrie N, Stock JM, Verdel C, Wernicke B (2003) Cenozoic evolution of Neotethys and implications for the causes of plate motions, *Geophysical Research Letters* 30 (20), 2036.
- Mirzaei Alavijeh H, Sinaeian F, Farzanegan E, Karimi P (2011) Characteristics of important Iranian earthquakes in 2008, *Asian Journal of civil engineering (building and housing)* 12 (5): 663-678.
- Nemati M, Hollingsworth J, Zhan Z, Bolourchi MJ, Talebian M (2013) Microseismicity and seismotectonics of the South Caspian Lowlands, NE Iran, *Geophysical Journal International* 193 (3): 1053-1070.
- Nemati M (2015) Intermediate-term variations in 200 years seismicity at the north of Iran, *Journal of Seismology* 19 (2): 585-605.
- Rastgoo M, Rahimi H, Romanelli F, Vaccari F, Panza GF (2018) Neo-deterministic seismic hazard assessment for Alborz Region, Iran, *Engineering Geology* 242: 70–80.
- Ritz JF, Nazari H, Ghassemi A, Salamati R, Shafei A, Solaymani S, Vernant P (2006) Active transtension inside central Alborz: a new insight into northern Iran-southern Caspian geodynamics, *Geology* 34: 477-480.
- Saber R, Caglayan A, Isik V (2018) Relative tectonic activity assessment and kinematic analysis of the North Bozghush fault Zone, NW Iran, *Journal of Asian Earth Sciences* 164: 219–236.
- Salmanlu A (2015) Spatio-temporal changes in the Late Cenozoic stress field of the Zanjan area: implications in the geodynamics of NW Iran, Thesis submitted for Master of Science in the field of Tectonics, *Bu-Ali Sina University*, Hamedan, Iran.
- Shahmirzae Jeshvaghani M, Darijani M (2014) Two-dimensional geomagnetic forward modeling using adaptive finite element method and investigation of the topographic effect, *Journal of Applied Geophysics* 105: 169–179.
- Solaymani Azad S, Dominguez S, Philip H, Hessami K, Forutan MR, Shahpassand Zadeh M, Ritz JF (2011) The Zandjan fault system: Morphological and tectonic evidences of a new active fault network in the NW of Iran, *Tectonophysics* 506 (1-4): 73–85.
- Solaymani Azad S, Nemati M, Abbassi MR, Foroutan M, Hessami Kh, Dominguez S, Bolourchi MJ, Shahpasandzadeh M (2019) Active-couple indentation in geodynamics of NNW Iran: Evidence from synchronous left- and right-lateral co-linear seismogenic faults in western Alborz and Iranian Azerbaijan domains, *Tectonophysics* 754: 1–17.
- Stocklin J, Eftekharneshad J (1969) Geological map of Zanjan quadrangle. *Geological Survey of Iran*, scale 1:250,000.
- Stocklin J (1974) Possible ancient continental margins in Iran, in Burke C, and Drake C, eds. The geology of continental margins, *Berlin, Springer, New York*, 873-887.
- Stocklin J, Setudehnia A (1977) Stratigraphic lexicon of Iran: Tehran, *Geological Survey of Iran*, 409 p.
- Taghipour K, Khatib MM, Heyhat MR, Shabani E, Vaezihir A (2018). Evidence for distributed active strike-slip faulting in NW Iran: The Maragheh and Salmas fault zones, *Tectonophysics* 742: 15–33.
- Toori M, Seyitoglu G (2014) Neotectonics of the Zanjan-Kazvin area, Central Iran: left lateral strike-slip induced restraining stepovers, *Turkish Journal of Earth Sciences* 23: 260-276.
- Zafarani H, Hassani B, Ansari A (2012) Estimation of earthquake parameters in the Alborz seismic zone, Iran using generalized inversion method, *Soil Dynamics and Earthquake Engineering* 42:197-218.